

Electronic Supply Information for:

Synthesis and Photophysical Properties of A “Face-to-Face” Stacked Tetracene Dimer

Heyuan Liu,^a Valerie M. Nichols,^b Li Shen,^a Setarah Jahansouz,^b Yuhan Chen,^a Kerry M. Hanson,^b Christopher J. Bardeen,^{*b} Xiyou Li,^{*a}

^a*Key Laboratory of Colloid and Interface Chemistry, Ministry of Education, Department of Chemistry, Shandong University, Jinan, China, 250100.*

^b*Department of Chemistry, University of California, Riverside, Riverside, CA 92521, USA*

Contents

1. CV (A) and DPV (B) plots of monomer **7** (Fig. S1).
2. Time-dependent change of the fluorescence spectra of dimer **6** in toluene exposed to light at room ambient condition (Fig. S2).
3. The fluorescence spectrum of dimer **6** in cyclohexane excited at 310 nm (Fig. S3).
4. The fluorescence decay of dimer **6** detected at different wavelengths in degassed toluene with B-field and without B-field (Fig. S4).
5. Copies of the ¹H NMR spectra and MALDI-TOF spectra of compound **5**, dimer **6** and monomer **7** (Fig. S5-S10).
6. The absorption spectra of monomer **7** and dimer **6** in toluene (Fig. S11).
7. The fluorescence decay of dimer **6** in toluene monitored at 535 nm (excited at 445 nm) (Fig. S12).
8. The fluorescence decay of dimer **6** in PS film monitored at 603 nm (excited at 445 nm) (Fig. S13).
9. A cartoon representation of the exciton states and processes involved in the fluorescence dynamics of dimer **6** (Fig. S14).
10. Minimized molecular structures for the different conformers of dimer **6**. (Fig. S15).
11. Simulated absorption spectra of different conformers of dimer **6**. (Fig. S16).
12. The final single point energy of different conformers of dimer **6** (Table. S1).
13. The Boltzmann-averaged UV-vis spectrum of dimer **6** (Fig. S17).

1. CV (A) and DPV (B) plots of monomer **7** in dichloromethane containing 0.1 M TBAP at room temperature.

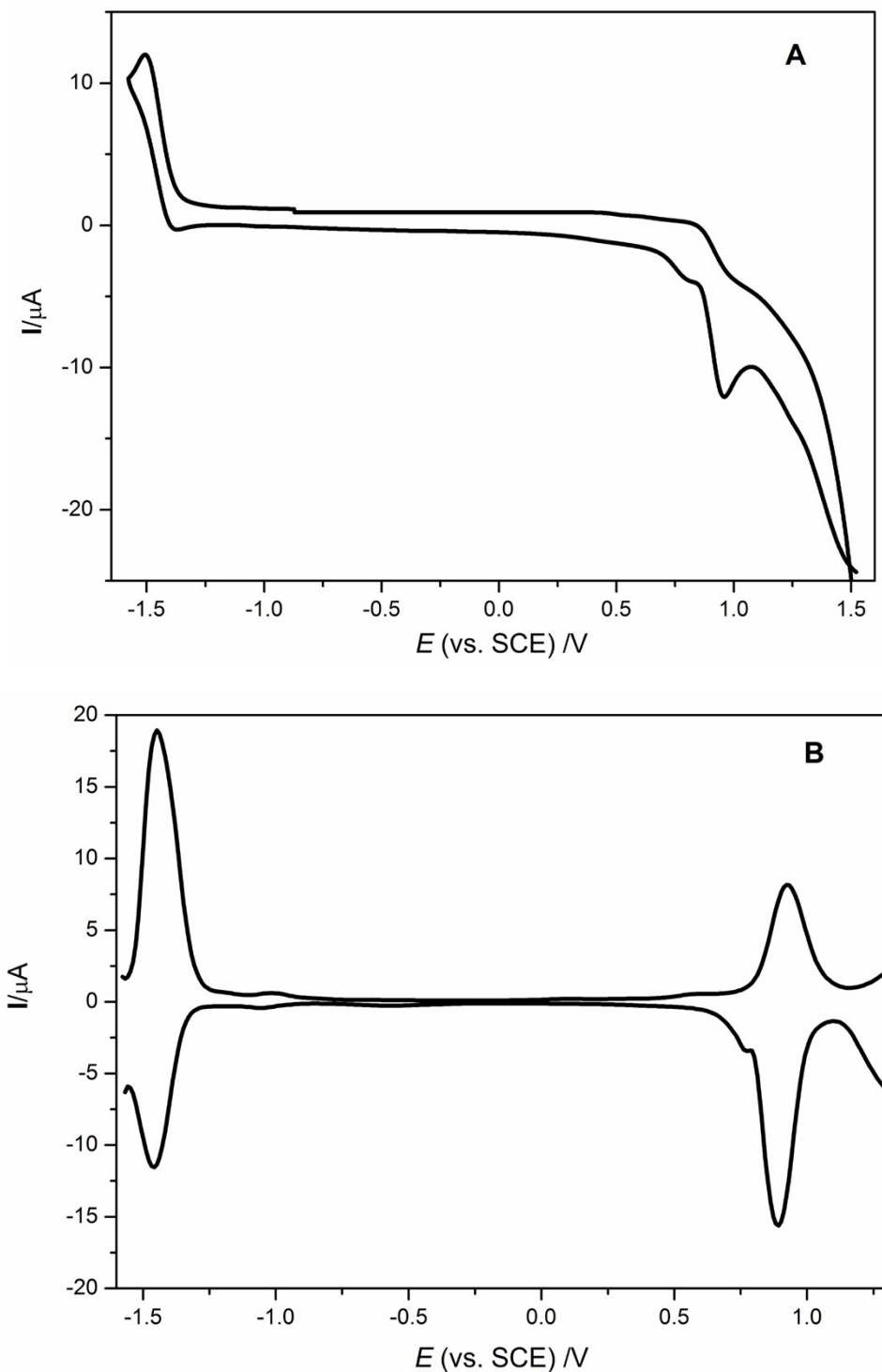


Fig. S1. CV (A) and DPV (B) plots of monomer **7** in dichloromethane containing 0.1 M TBAP.

2. Time-dependent change of the fluorescence spectra of dimer **6** in toluene exposed to light at room ambient condition.

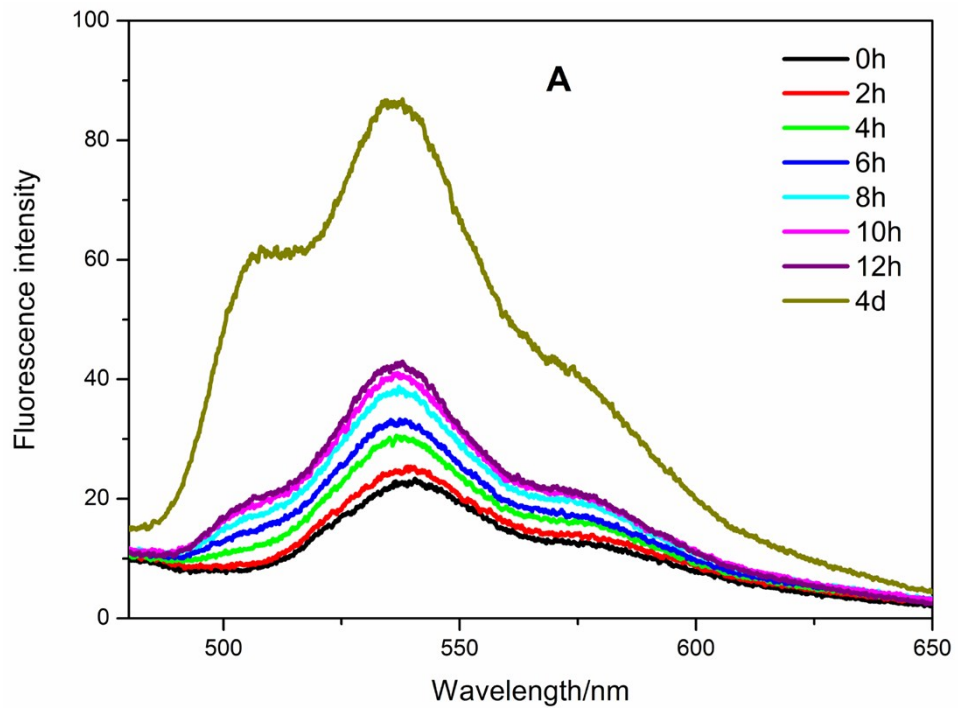


Fig. S2. Time-dependent change of the fluorescence spectra of dimer **6** in toluene exposed to light at room ambient condition.

3. The fluorescence spectrum of dimer **6** in cyclohexane excited at 310 nm.

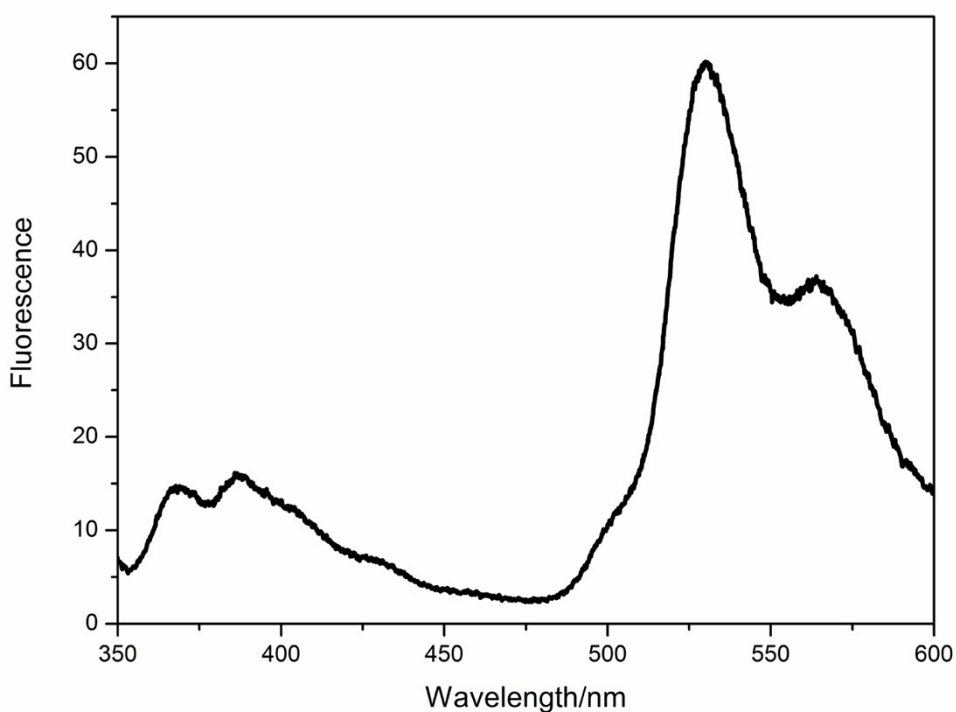


Fig. S3 The fluorescence spectrum of dimer **6** in cyclohexane excited at 310 nm.

4. The fluorescence decay of dimer **6** detected at different wavelengths in degassed toluene with B-field and without B-field.

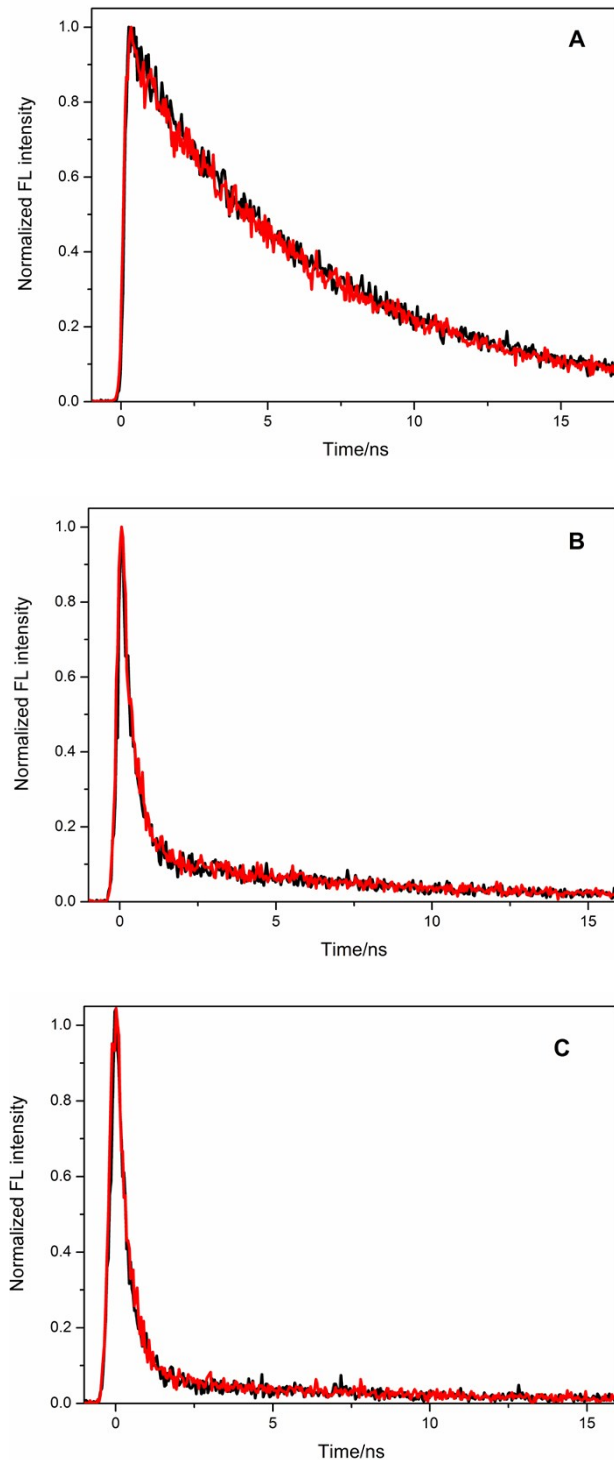


Fig. S4 The fluorescence decay of dimer **6** detected at 508 nm (A), 600 nm (B) and 625 nm (C) in degassed toluene with B-field (black) and without B-field (red).

5. Copies of the ^1H NMR spectra and MALDI-TOF spectra of compound **5**, dimer **6** and monomer **7**.

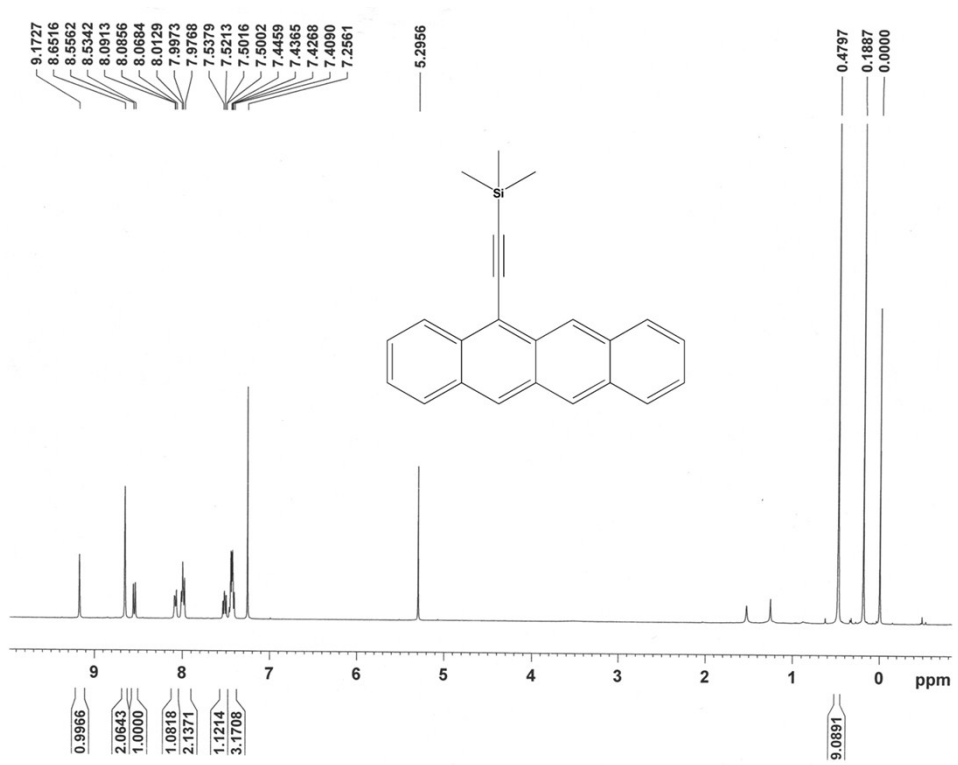


Fig. S5. The ^1H NMR spectrum of compound **5**.

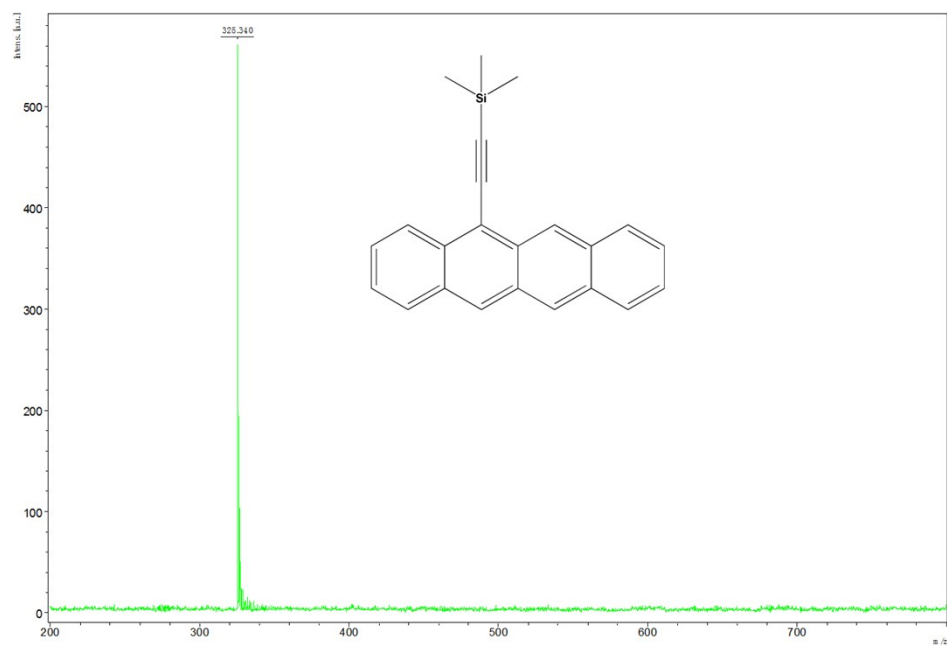


Fig. S6. The MALDI-TOF spectrum of compound **5**.

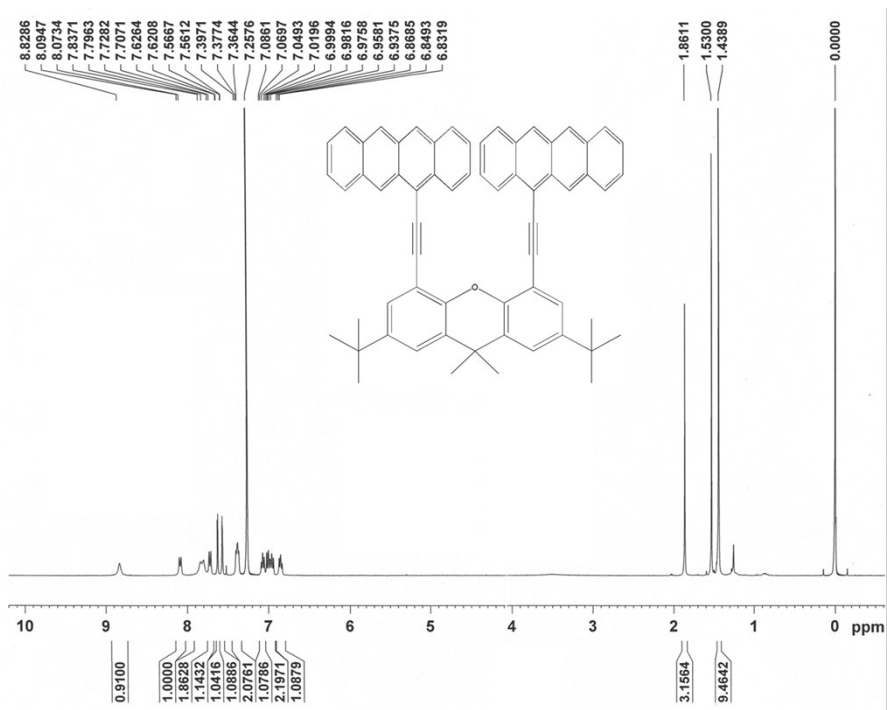


Fig. S7. The ^1H NMR spectrum of dimer **6**.

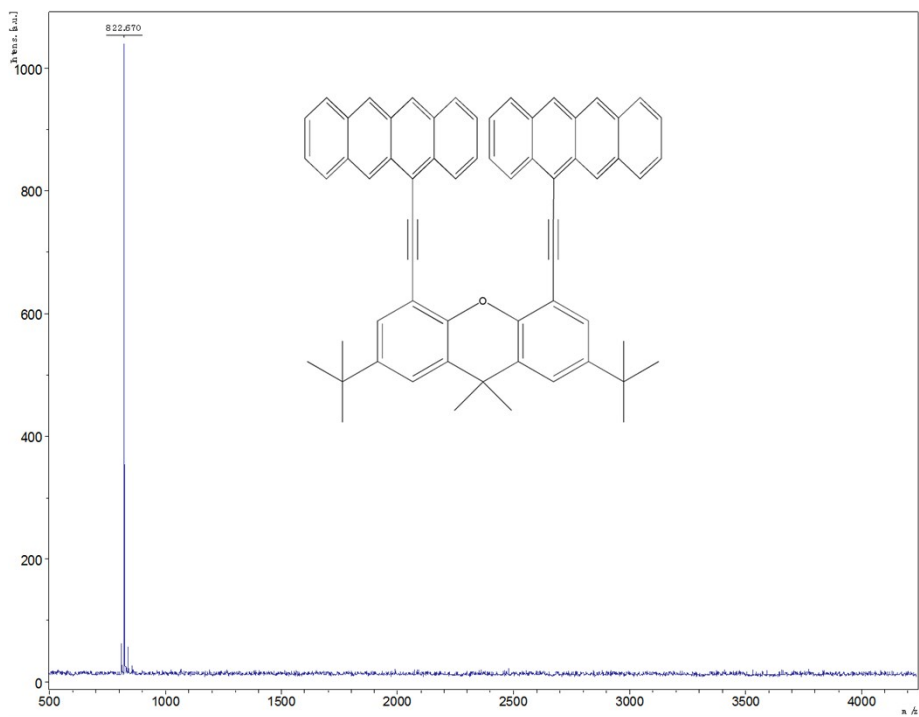


Fig. S8. The MALDI-TOF spectrum of dimer **6**.

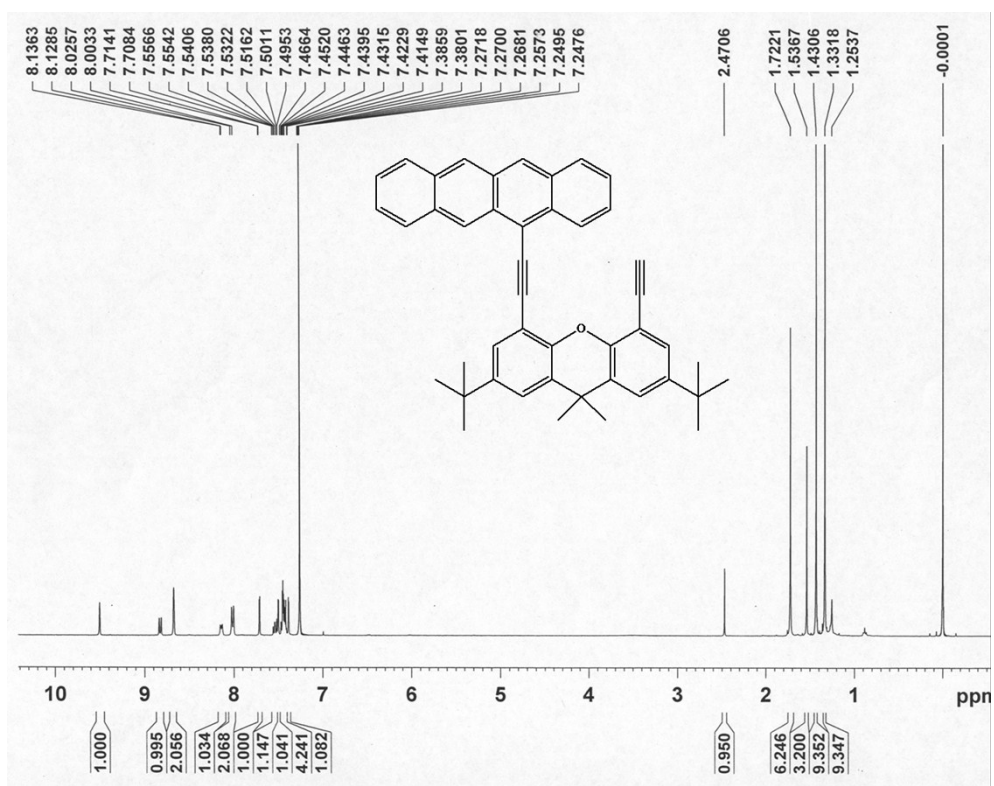


Fig. S9. The ^1H NMR spectrum of monomer 7.

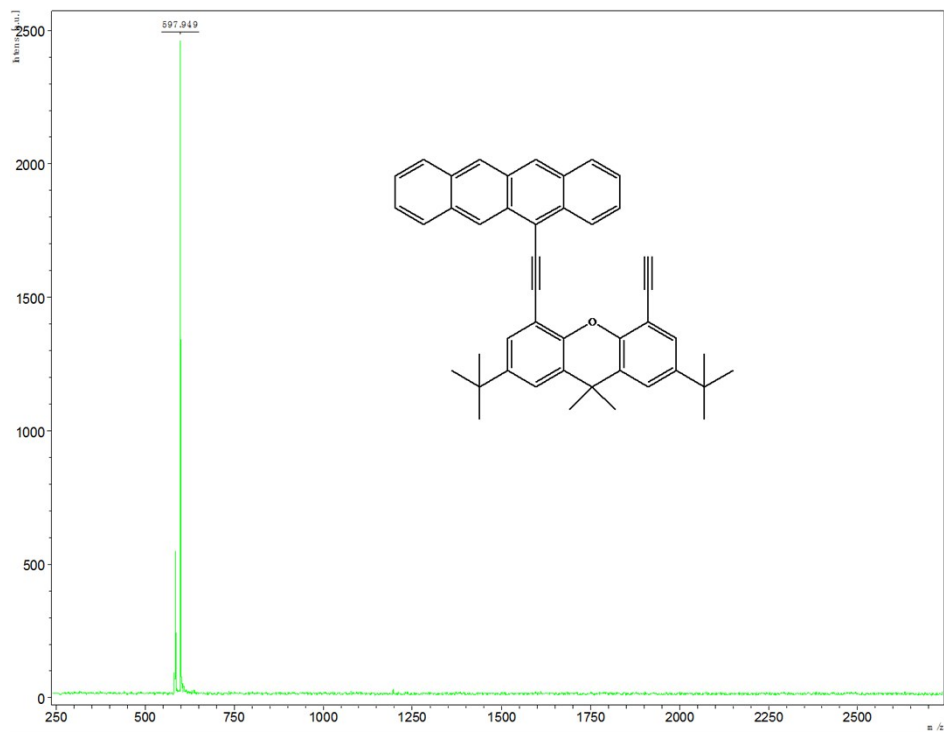


Fig. S10. The MALDI-TOF spectrum of monomer 7.

6. The absorption spectra of monomer **7** and dimer **6** in toluene.

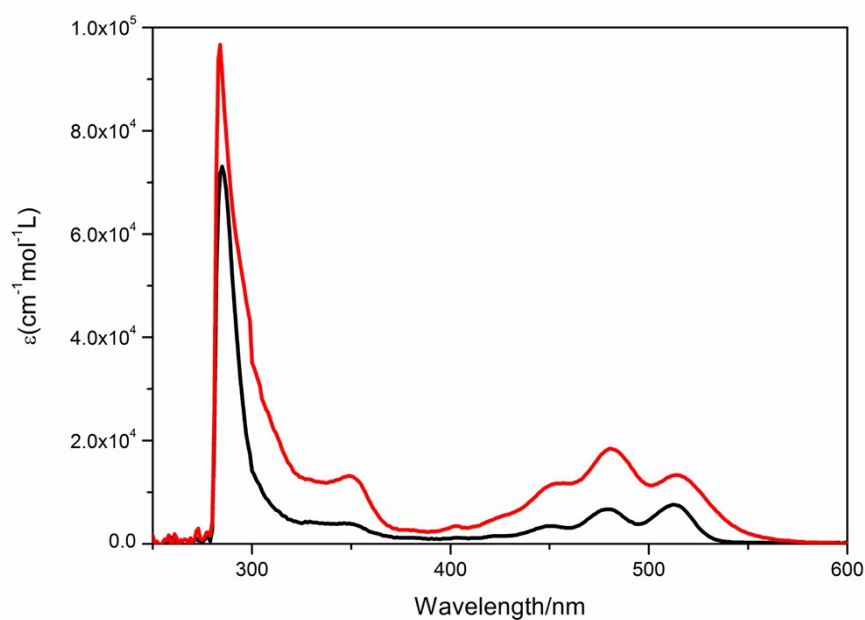


Fig. S11. The absorption spectra of monomer **7** (black) and dimer **6** (red) in toluene.

7. The fluorescence decay of dimer **6** in toluene monitored at 535 nm (excited at 445 nm).

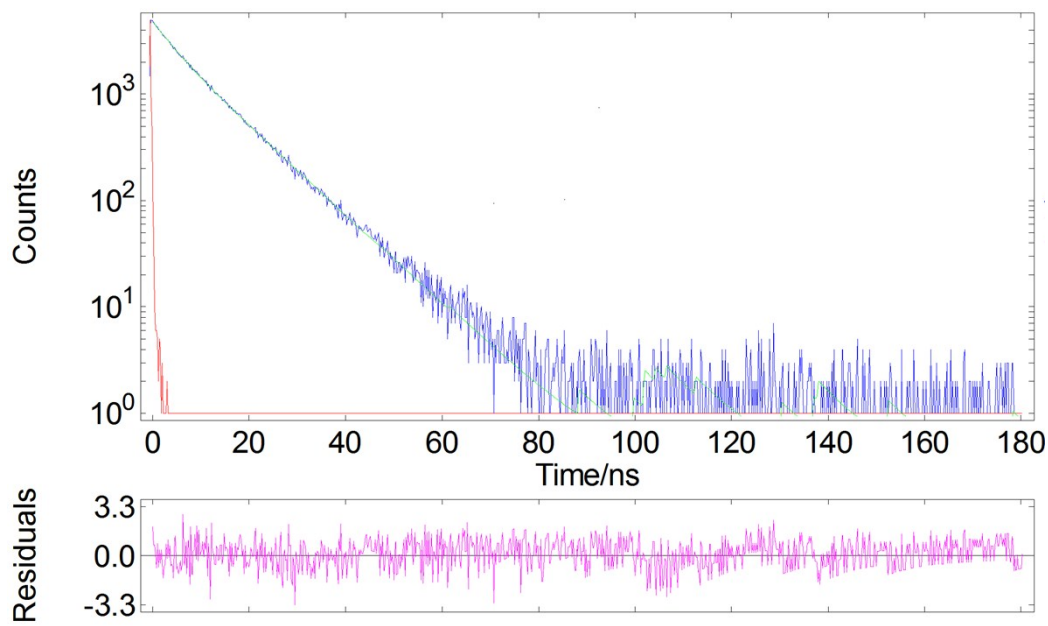


Fig. S12. The fluorescence decay (blue line) of dimer **6** in toluene monitored at 535 nm (excited at 445 nm). Also shown is the fit to the date (green line).

8. The fluorescence decay of dimer **6** in PS film monitored at 603 nm (excited at 445 nm).

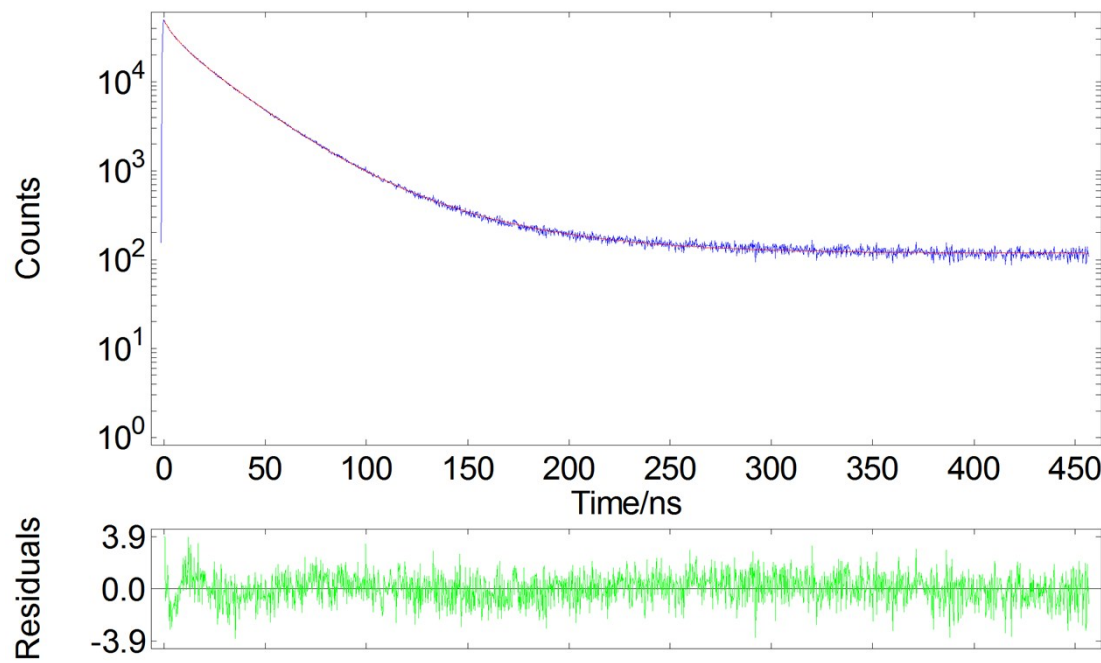
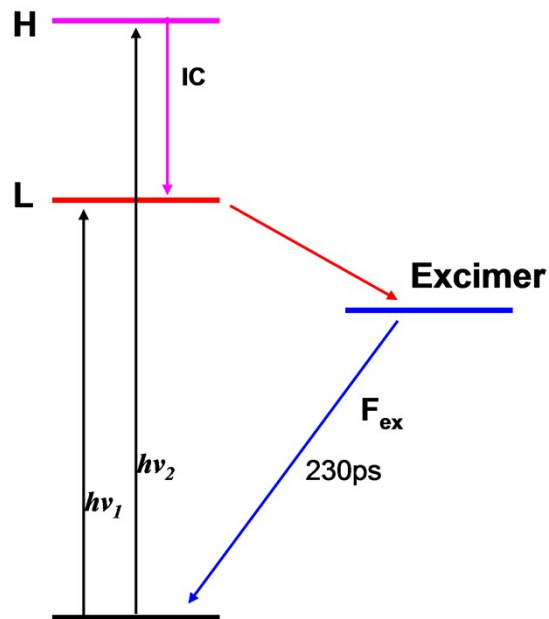


Fig. S13. The fluorescence decay (blue line) of dimer **6** in PS film monitored at 603 nm (excited at 445 nm). Also shown is the fit to the date (red line).

9. A cartoon representation of the exciton states and processes involved in the fluorescence dynamics of dimer **6**.



H high exciton state; **L** Low exciton state; **IC** internal conversion;
 F_{ex} excimer fluorescene; $h\nu_1$ and $h\nu_2$, excitation light.

Fig. S14. A cartoon representation of the exciton states and processes involved in the fluorescence dynamics of dimer **6**

10. Minimized molecular structures for the different conformers of dimer **6**.

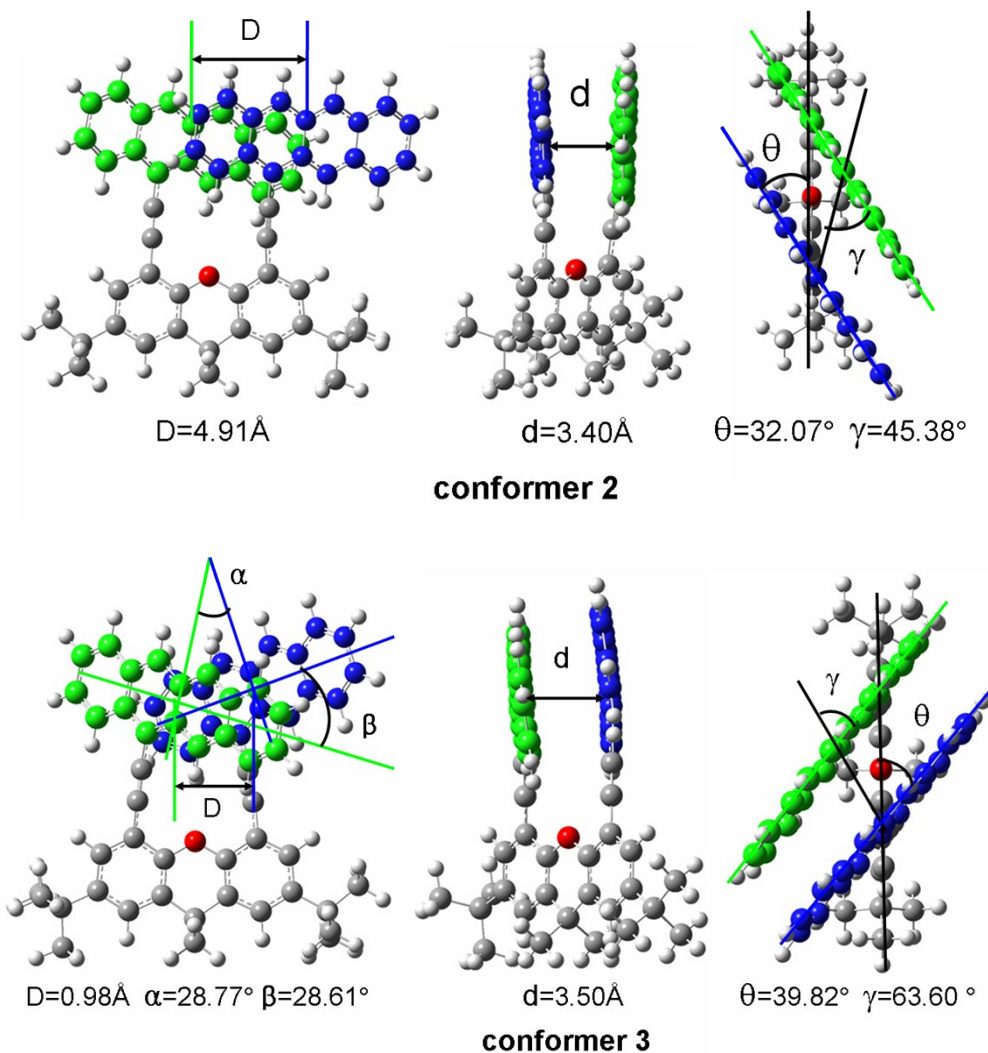


Fig. S15. Minimized molecular structures for the different conformers of dimer **6** (The structure of conformer **1** was shown in the main text).

11. Simulated absorption spectra of different conformers of dimer **6**.

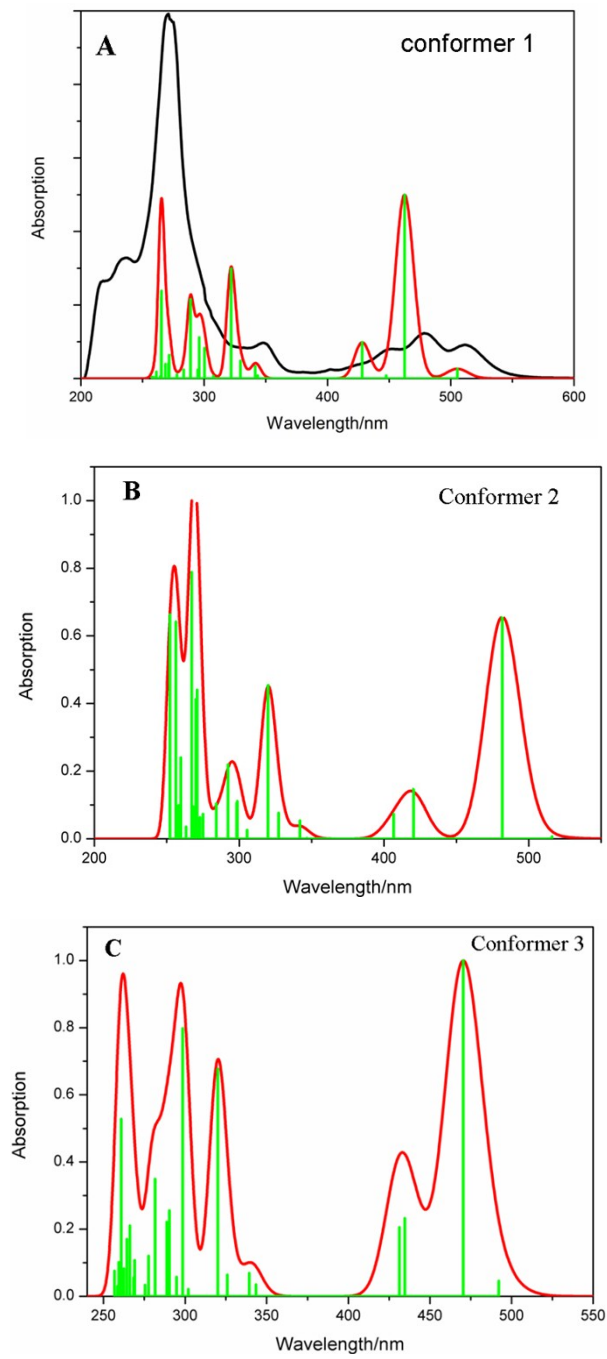


Fig. S16. Simulated (red) and experimental (black) absorption spectra of different conformers of dimer **6** (the structures are shown in Fig. S15). Bars indicate the contribution modes. The calculation was done on the level of ω -B97XD^{S1-3}/6-31G(d) in the Gaussian 09^{S4} program package in vacuum.

12. The final single point energies of different conformers of dimer **6**.

Table S1. Final single point energies of different conformers of dimer **6**.

conformer	1	2	3
Final single point energy(kcal/mol)	-1.572059×10^6	-1.572054×10^6	-1.572057×10^6

13. The Boltzmann-averaged UV-vis spectrum of dimer **6**.

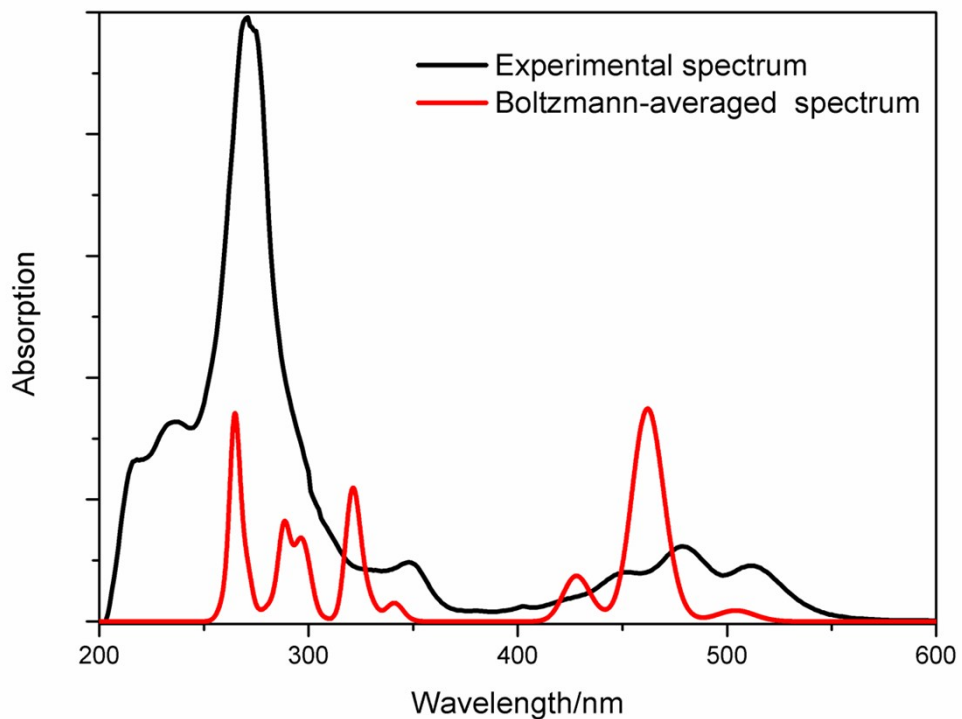


Fig. S17. The Boltzmann-averaged UV-vis spectrum of dimer **6** (red line). The Boltzmann-averaged UV-vis spectrum was obtained from SpecDis Manual program^{S5}.

Reference

- S1 J. D. Chai and M. Head-Gordon, *J. Chem. Phys.*, 2008, **128**, 1–6.
- S2 J. D. Chai and M. Head-Gordon, *Phys. Chem. Chem. Phys.*, 2008, **10**, 6615–6620.
- S3 P. J. Vallett, J. L. Snyder and N. H. Damrauer, *J. Phys. Chem. A*, 2013, **117**, 10824–10838.
- S4 Gaussian 09, Revision B.01, M. J. Frisch, G. W. Trucks, H. B. Schlegel, G. E. Scuseria, M. A. Robb, J. R. Cheeseman, G. Scalmani, V. Barone, B. Mennucci, G. A. Petersson, H. Nakatsuji, M. Caricato, X. Li, H. P. Hratchian, A. F. Izmaylov, J. Bloino, G. Zheng, J. L. Sonnenberg, M. Hada, M. Ehara, K. Toyota, R. Fukuda, J. Hasegawa, M. Ishida, T. Nakajima, Y. Honda, O. Kitao, H. Nakai, T. Vreven, J. A. Montgomery, Jr., J. E. Peralta, F. Ogliaro, M. Bearpark, J. J. Heyd, E. Brothers, K. N. Kudin, V. N. Staroverov, T. Keith, R. Kobayashi, J. Normand, K. Raghavachari, A. Rendell, J. C. Burant, S. S. Iyengar, J. Tomasi, M. Cossi, N. Rega, J. M. Millam, M. Klene, J. E. Knox, J. B. Cross, V. Bakken, C. Adamo, J. Jaramillo, R. Gomperts, R. E. Stratmann, O. Yazyev, A. J. Austin, R. Cammi, C. Pomelli, J. W. Ochterski, R. L. Martin, K. Morokuma, V. G. Zakrzewski, G. A. Voth, P. Salvador, J. J. Dannenberg, S. Dapprich, A. D. Daniels, O. Farkas, J. B. Foresman, J. V. Ortiz, J. Cioslowski and D. J. Fox, Gaussian, Inc., Wallingford CT, 2010.
- S5 T. Bruhn, A. Schaumlöffel, Y. Hemberger and G. Bringmann, SpecDis, Version 1.62, University of Wuerzburg, Germany, 2014.